# FINAL REPORT - PHASE I

# TUNABLE HIGH $T_c$ SUPERCONDUCTING INFRARED DETECTORS

Sponsored by:
Defense Advanced Research Projects Agency (DoD)
Defense Small Business Innovation Research Program
ARPA Order No. 5916
Issued by U.S. Army Missile Command Under
Contract No. DAAH01-88-C-0745



Principal Investigator: James D. Klein
Phone Number (617) 769-9450

EIC Laboratories, Inc.
111 Downey Street
Norwood, Massachusetts 02062

Effective Date of Contract - August 23, 1988
Contract Expiration Date - February 28, 1989

Reporting Period: August 23, 1988 to February 28, 1989

## DISCLAIMER

"The views and conclusions contained in this document are those of the authors and should not be interpreted as representing the official policies, either expressed or implied, of the Defense Advanced Research Projects Agency or by the U.S. Government."

UNCLASSIFIED

SECURITY CLASSIFICATION OF THIS PAGE

# REPORT DOCUMENTATION PAGE

| | |
|---|---|
| 1a. REPORT SECURITY CLASSIFICATION<br>UNCLASSIFIED | 1b. RESTRICTIVE MARKINGS |
| 2a. SECURITY CLASSIFICATION AUTHORITY | 3. DISTRIBUTION/AVAILABILITY OF REPORT |
| 2b. DECLASSIFICATION/DOWNGRADING SCHEDULE | |
| 4. PERFORMING ORGANIZATION REPORT NUMBER(S)<br>C-981F | 5. MONITORING ORGANIZATION REPORT NUMBER(S) |
| 6a. NAME OF PERFORMING ORGANIZATION<br>EIC Laboratories, Inc.<br>6b. OFFICE SYMBOL (If applicable) | 7a. NAME OF MONITORING ORGANIZATION<br>U.S. Army Missile Command |
| 6c. ADDRESS (City, State, and ZIP Code)<br>111 Downey Street<br>Norwood, Massachusetts 02062 | 7b. ADDRESS (City, State, and ZIP Code)<br>AMSMI-PC-BFA/DARPA PROJECT OFFICE<br>Redstone Arsenal, AL 35898-5244 |
| 8a. NAME OF FUNDING/SPONSORING ORGANIZATION<br>8b. OFFICE SYMBOL (If applicable) | 9. PROCUREMENT INSTRUMENT IDENTIFICATION NUMBER<br>DAAH01-88-C-0745 |
| 8c. ADDRESS (City, State, and ZIP Code) | 10. SOURCE OF FUNDING NUMBERS<br>PROGRAM ELEMENT NO. / PROJECT NO. / TASK NO / WORK UNIT ACCESSION NO. |

11. TITLE (Include Security Classification)
TUNABLE HIGH $T_C$ SUPERCONDUCTING INFRARED DETECTORS

12. PERSONAL AUTHOR(S) James D. Klein

| 13a. TYPE OF REPORT | 13b. TIME COVERED | 14. DATE OF REPORT (Year, Month, Day) | 15. PAGE COUNT |
|---|---|---|---|
| Final Report | FROM Aug 88 TO Feb 89 | 1989 February | 28 |

16. SUPPLEMENTARY NOTATION

| 17. COSATI CODES | | | 18. SUBJECT TERMS (Continue on reverse if necessary and identify by block number) |
|---|---|---|---|
| FIELD | GROUP | SUB-GROUP | Key Words: Superconductors, Infrared Detectors, $YBa_2Cu_3O_7$, Ion Conductors, Thin Film. (JES) |
| | | | |
| | | | |

19. ABSTRACT (Continue on reverse if necessary and identify by block number)

This program is aimed at the development of a superconductor based infrared detector in which sensitivity is optimized through control over composition and microstructure. Cation composition and thin film morphology are to be determined precisely in the thin film deposition process. The superconducting thin film is to have an oriented polycrystalline microstructure to achieve Josephson junction behavior directly through the anisotropic superconducting properties of $YBa_2Cu_3O_{7-x}$. The deposition substrate will be an oxygen ion conductor to permit continuous and controlled adjustment of the superconductor's oxygen stoichiometry. Since the properties of the new oxide superconductors are so dependent on the oxygen stoichiometry of the crystal lattice, such a device can be tuned for various operating conditions. By providing a means for adjusting the transition temperature of the device after depositions the limitations placed on previous superconducting infrared detectors, such as the need for demanding temperature control during operation, will be circumvented. Phase I was concerned with defining film deposition conditions and determining the oxygen transport characteristics of the superconducting films on the chosen substrate.

| 20. DISTRIBUTION/AVAILABILITY OF ABSTRACT | 21. ABSTRACT SECURITY CLASSIFICATION |
|---|---|
| ☒ UNCLASSIFIED/UNLIMITED ☐ SAME AS RPT. ☐ DTIC USERS | UNCLASSIFIED |
| 22a. NAME OF RESPONSIBLE INDIVIDUAL<br>Charles R. Piner | 22b. TELEPHONE (Include Area Code)<br>(205) 876-3836 / 22c. OFFICE SYMBOL |

DD FORM 1473, 84 MAR 83 APR edition may be used until exhausted. All other editions are obsolete

SECURITY CLASSIFICATION OF THIS PAGE

☆ U.S. Government Printing Office: 1986—607-044

TABLE OF CONTENTS

LIST OF FIGURES

LIST OF FIGURES
(Continued)

# 1.0 INTRODUCTION

With ever increasing demands on surveillance, target acquisition, and tracking, future space and ground-based ballistic missile defense systems will require increasingly effective means of infrared detection. High $T_c$ superconductivity should permit the operation of highly sensitive detectors once the necessary control over composition and microstructure are achieved. Although advances in the deposition and patterning of high $T_c$ materials for circuit applications have been forthcoming, the implementation of ceramic superconductors in detection devices has been hindered by imprecise control of stoichiometry and structure. Although the oxide superconductors are readily capable of operation above liquid nitrogen temperature, they exhibit several materials characteristics that must be properly coordinated with device parameters to realize practical utilization. Anisotropies in critical current and critical field presently limit the adaptability of these materials in electromagnet conductor applications. Additional restraints may be imposed by the tendency of nonsuperconducting phases at grain boundaries to create Josephson junctions between adjacent crystals. The stoichiometry-dependent electronic properties will dictate precise control of fabrication methods to achieve desired properties in feasible devices. In the case of detectors, a device possessing maximum sensitivity near a conveniently maintained temperature may be more useful than one exhibiting the highest critical temperature. These considerations are best met by devices that are enhanced rather than compromised by materials characteristics.

## 1.1 Device Concept

A suitable device will exhibit the desired Josephson junction characteristics over the chosen temperature range as determined by direct manipulation of stoichiometry and structure during the production sequence. However, the demonstration of a practical device requires the combination of emerging fabrication techniques with innovative device designs in order to free superconducting detectors from the precise temperature control previously required for superconducting bolometers. Three major innovations are proposed: [1] precise stoichiometry and morphology control through specific deposition protocol, [2] in situ development of random Josephson junction arrays by the formation of an oriented polycrystalline film of a highly anisotropic superconductor, and [3] incorporation of an oxygen ion conductor substrate to permit the continuous control of superconducting properties through variation of the oxygen stoichiometry. The combination of precise deposition, oriented polycrystalline microstructure, and dynamically adjustable stoichiometry should permit the operation of a highly sensitive, predictable, and tunable infrared detector.

Such a device will have the following characteristics:

- Highly developed deposition techniques can readily provide oriented homogeneous thin films of appropriate cation stoichiometry and crystal morphology without post deposition anneals.

- An oriented polycrystalline film will directly provide random Josephson junction behavior through the anisotropic superconducting properties inherent in this class of materials.

- The use of an oxygen ion conductor as the substrate will permit active adjustment of the superconducting properties through the application of an external voltage to set oxygen content after all necessary device layers have been deposited. Therefore, the behavior of the device will be tunable and/or correctable for optimum operation.

- The resulting tunable nature of the superconducting film imparts great flexibility to the device fabrication process resulting in:
  - the ability to configure devices of different oxygen stoichiometries from a uniform set of thin film structures;
  - ready generation of gradients in detector element response through variations in oxygen stoichiometry.
- Since the superconductor film will not be directly exposed to ambient gases during the setting of the oxide stoichiometry, the need for stringent atmosphere control is removed.

The combination of these features will result in a truly novel device having adaptable infrared characteristics. The implementation of the new high-$T_c$ superconductors in practical infrared detectors is dependent on the successful exploitation of the properties inherent to this class of materials. The polycrystalline variable-stoichiometry technology proposed embraces the anisotropy and stoichiometry-dependence of the ceramic superconductors as functional device attributes.

## 1.2 Materials Considerations

The most advantageous configuration for a high $T_c$ infrared detector is anticipated to be a thin film within which a multitude of Josephson junctions are defined. Granular films of high $T_c$ superconductor in a nonsuperconducting matrix have been obtained through a morphology of $YBa_2Cu_3O_7$ (YBCO) crystals embedded in Y-Ba-Cu-O of nonstoichiometric composition (1). Although the superconducting transition was depressed and very broad, the device responded to radiation from the visible to the far infrared. An interesting characteristic was an apparent peaking of signal strength near the 35 K onset temperature of the transition. More recent experiments on epitaxial $YBa_2Cu_3O_7$ films suggest that rapid nonbolometric responses are possible if the grain boundaries in the film are artificially weakened (2). Extremely rapid "photolytic" responses below the transition temperature have been observed in transparent epitaxial films (3). This suggests that, in the absence of preexisting weak links, the incident radiation must penetrate the entire film depth to prevent unaffected underlying material from shorting the electrical signal. A thin film structure comprised of high critical current density regions separated by thin junction surfaces is needed for high performance infrared detectors. The high critical current areas will provide fast low noise transmission of the signals arising from radiation-impaired superconductivity at the junctions.

When deposited with the correct cation stoichiometry and crystallographic orientation, $YBa_2Cu_3O_7$ films exhibit critical temperatures approaching 95 K and critical current densities of more than $1 \times 10^6$ A/cm$^2$ at 81 K (4). The importance of cation stoichiometry is derived from simple phase diagram ramifications. Reference to the CuO-BaO-$YO_{1.5}$ ternary phase diagram reveals several Y-Ba-Cu and binary oxides, each with its own well defined cation ratios (5). However, since only $YBa_2Cu_3O_{7-x}$ is superconducting, the effect of improper cation stoichiometry is to introduce insulating or semiconducting phases in the microstructure. Although oxygen content is often set during post-deposition heat treatments, precise cation stoichiometry must be achieved during deposition. The electronic circuit applications of single crystal epitaxial films are obvious. However, successful detector implementation requires a convenient means for creating a system of localized Josephson junctions.

The anisotropy and oxygen stoichiometry dependence of the YBCO superconducting properties provide unique opportunities for developing the necessary weak link structure after film deposition. Many investigators have observed a tendency for the critical current density to be sharply reduced in sintered samples (6,7) which by their nature are a conglomeration of single crystals of generally random orientation. Magnetization experiments that define a great enhancement in critical current density upon grinding sintered samples to powder (8) indicate that the connection between randomly oriented grains is responsible for the poor behavior of sintered pellets. Thus, it is obvious that a polycrystalline film will contain grains of relatively high critical current density surrounded by grain boundaries of significantly lower critical current density. Recently, the dependence of grain boundary critical current density on the misorientation of epitaxial bicrystals has been defined. Tilt angles of 15 degrees between adjacent grains reduced critical current by a factor of 100 (9). The desired polycrystal morphology can be achieved through the influence of a noble metal interlayer. Elevated temperature deposition of the high $T_c$ superconductor 123 ErBaCuO atop a textured noble metal film yields an oriented polycrystalline superconductor with a smooth surface (10). Since noble metals have little tendency to react with high $T_c$ superconductors, the interlayer effectively transfers the epitaxy from the substrate while chemically isolating the substrate from the superconductor.

The $YBa_2Cu_3O_7$-based superconductors are similar to many electronic oxides in that their transport properties are strongly dependent on the oxygen deficiency in the lattice (11,12). Even after the Y, Ba, and Cu cation stoichiometries have been set during fabrication the electronic properties may be enhanced or degraded by exposure to oxidizing or reducing atmospheres. This "breathing" of oxygen can even be performed cyclically so that $YBa_2Cu_3O_{7-x}$ has been termed "a line compound intercalated by oxygen vacancies" (12). Although the results of different investigators differ somewhat, the apparent effect of oxygen stoichiometry on $T_c$ is given in Figure 1. Specifically, if a transition temperature between 90 and 60 K is desired, the average Cu ion valence should be lowered from the nominal value of 2.33 in $YBa_2Cu_3O_7$. This dependence of the superconducting transition on oxygen content probably explains most of the variation in properties observed by early investigators. More importantly, it implies that deliberate control over the superconducting properties is available if the oxygen stoichiometry can be successfully and consistently managed. It also becomes apparent that a range of critical temperatures can be incorporated into a single device simply by establishing a range of oxygen stoichiometries.

Manipulation of the oxygen stoichiometry in YBCO films requires a manageable method for inserting or removing oxygen. To date, most investigators have accomplished changes in oxygen content by annealing samples in controlled atmosphere furnaces. Decreasing the critical temperature of the $YBa_2Cu_3O_x$ orthorhombic phase from 90 to 60 K requires that x be reduced from 6.9 to 6.7. Analysis of equilibrium data (11) shows that this corresponds to a variation of more than two orders of magnitude in equilibrium oxygen partial pressure at any given temperature. Therefore, the incorporation of a range of critical temperatures in a device cannot be readily achieved by establishing equilibrium in a controlled atmosphere furnace.

The realization of designed gradient stoichiometries becomes feasible if a control voltage across an ion conducting solid electrolyte rather than an ambient atmosphere is utilized to determine oxygen content. The operation of an oxygen ion conductor is most easily understood by considering fuel cell applications. Stabilized zirconia fuel cells produce a voltage through the driving force provided by differing oxygen partial pressures (13). The cell diagram with platinum electrodes is

$$\begin{array}{c|c|c} \text{Pt, } O_2 \\ \text{at high } P'(O_2) & ZrO_2 - Y_2O_3 & \begin{array}{c}\text{Pt, } O_2 \\ \text{at low } P''(O_2)\end{array} \end{array}$$

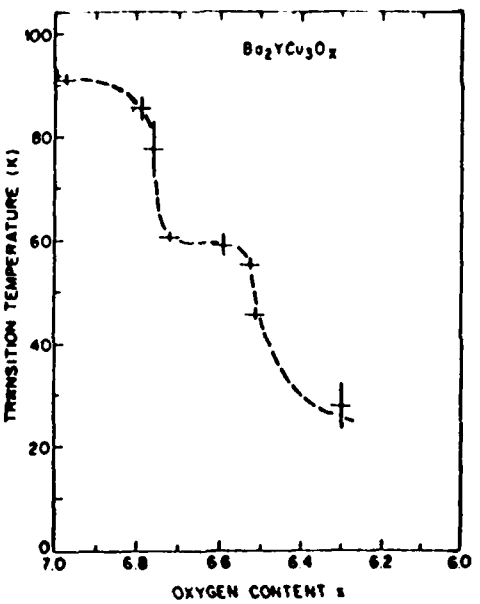


Figure 1. The trend of the critical temperature of $YBa_2Cu_3O_x$ as a function of oxygen content (after 11).

There exists an obvious driving force for oxygen at the high partial pressure $P'(O_2)$ to move to the lower partial pressure $P''(O_2)$. If the electrolyte were permeable to $O_2$ molecules, this would occur without producing any recoverable work. However, the $Y_2O_3$ stabilized $ZrO_2$ is not permeable to $O_2$ but will pass $O^=$ ions. It is then required that the oxygen (i) be ionized (gaining electrons) at $P'(O_2)$, (ii) diffuse through the electrolyte, and (iii) reform molecules (losing electrons) at $P''(O_2)$. If stabilized zirconia were a good conductor of electrons, both $e^-$ and $O^=$ would pass (in opposite directions) through the electrolyte while producing no recoverable work. Fuel cell operation demands that the electrolyte pass $O^=$ ions while being a poor conductor of electrons. The electrons are then subject to a driving force (electrical potential) which will result in a current through an external circuit.

The voltage corresponding to the ratio of oxygen partial pressures is easily calculated from the reaction conditions. The net chemical reaction is

$$O_2 \text{ (at high } P'(O_2)) \Longrightarrow O_2 \text{ (at low } P''(O_2))$$

The open circuit voltage V is given by

$$V = \frac{R\,T \ln (P'/P'')}{4\,e^-/O_2\,N_A\,e}$$

It is apparent that high voltages result from high $P'(O_2)/P''(O_2)$ ratios and high operating temperatures. When stabilized $ZrO_2$ electrolytes are employed as oxygen pumps in vacuum systems (14,15), the voltage maintained across the electrodes controls the difference in the chemical potential of the oxygen across the two sides of the electrolyte. For example, as shown in Figure 2, setting the equilibrium oxygen content x between 6.7 and 6.9 in $YBa_2Cu_3O_x$ will require control voltages of 0.15 to 0.08 volts if one atmosphere of oxygen is the supply atmosphere in a

400°C furnace. Since oxygen mobility in $YBa_2Cu_3O_x$ is negligible below 350°C (16), the oxygen content set by elevated temperature operation of the ion conductor is preserved at ambient and cryogenic temperatures.

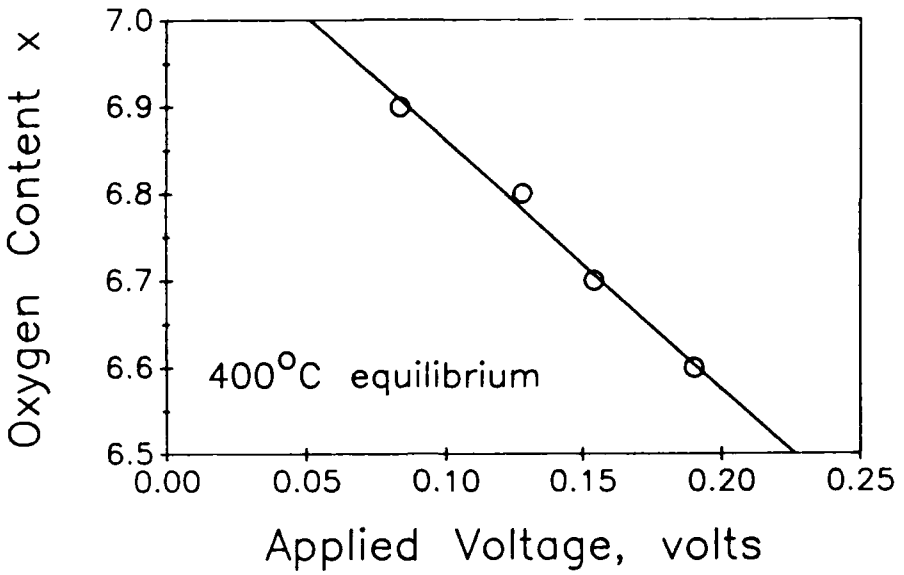


Figure 2. The oxygen content x in $YBa_2Cu_3O_x$ as a function of the voltage across an oxygen conductor supplied by one atmosphere of oxygen at 400°C.

### 1.3 Device Geometry

Although a variety of designs are possible using the oxygen ion conductor substrate technology, the relatively simple layered structure shown at the top of Figure 3 was originally proposed for this project. However, in light of the films developed in Phase I the higher performance design shown in the bottom of Figure 3 is now preferred.

The improvement lies in the utilization of an oriented polycrystalline layer in place of the randomly oriented grains depicted in the original device. This should enhance the available signal by allowing a higher superconducting critical current when the device is not illuminated. Also, the extension of the grain boundary weak links through the entire depth of the film precludes the shunting of the signal by subsurface superconducting grains.

The buildup of layers begins with the coating of both sides of the yttria stabilized zirconia (YSZ) oxygen ion conductor substrate with thin films of a noble metal. The bottom layer merely provides one electrode for the electrochemical pumping of oxygen through the YSZ substrate by the application of an externally controlled voltage. The noble metal interlayer has three important functions: [1] a second electrode for the oxygen ion conductor cell, [2] an oriented substrate for the superconductor deposition, and [3] a diffusion barrier between the YSZ substrate and the YBCO superconductor. The oriented polycrystalline morphology of the $YBa_2Cu_3O_7$ superconductor is an intentional result of the epitaxy originated in the YSZ substrate being transferred by the polycrystalline noble metal interlayer. A noble metal grid placed on top of the superconductor allows contact to the junction structure provided by the stoichiometrically adjusted grain boundaries. The top layer serves multiple functions in that it is both an infrared window and a barrier layer isolating the superconductor from its environment. An important virtue of this design is the ability to set the

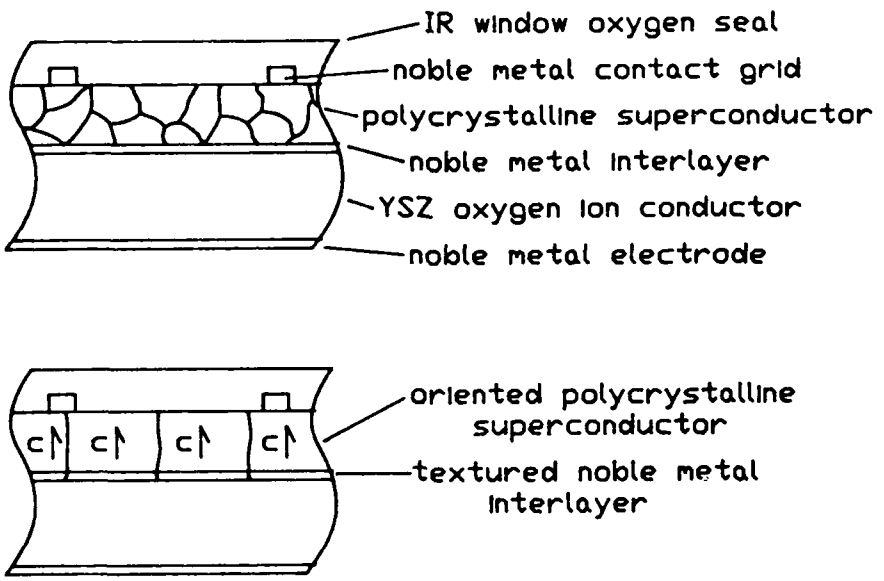


Figure 3. The original (upper) and revised (lower) geometries structure of a demonstration infrared detector based on a tunable oriented polycrystalline superconducting film. There are six distinct layers.

oxide stoichiometry of the superconductor without precise control of the furnace atmosphere. The control voltage across the YSZ dictates the ratio of device oxygen partial pressure to that of an ambient furnace atmosphere.

## 2.0 RESULTS

The phase diagram of the Y-Ba-Cu oxide system requires that the cation stoichiometry of the $YBa_2Cu_3O_7$ superconducting phase be reproduced rather precisely in order to achieve good transport properties in deposited films. As might be suspected from the differences in the melting points of Y (1799 K), Ba (1002 K), and Cu (1358 K), the sputtering characteristics of the three cation species differ markedly. This results in varying degrees of susceptibility to undesirable negative ion resputtering from the substrate. These differences are manifested in the great difficulty encountered in consistently depositing films of the necessary stoichiometry. Since the sputtering characteristics of each deposition arrangement are different, an appreciable portion of the Phase I effort was expended in determining the role of sputtering variables on the stoichiometry, orientation, and morphology of the deposited films.

### 2.1 The Effect of Sputtering Variables

The thin films produced in the Phase I program were deposited by rf magnetron sputtering on single crystal ceramic substrates. To minimize the effects of negative ion resputtering a substrate arrangement similar to that of Sandstrom et al. (17) was chosen. As shown in Figure 4, the substrate was placed to the side of the target centerline at an inclination of 30 degrees to the horizontal. The most important feature of this configuration is the removal of the substrate surface from the sputtering plasma. This largely precludes resputtering from the substrate surface by negative ions in the plasma. The uniformity of the film composition and thickness across the face of the substrate was insured by continuously rotating the holder about its axis during deposition.

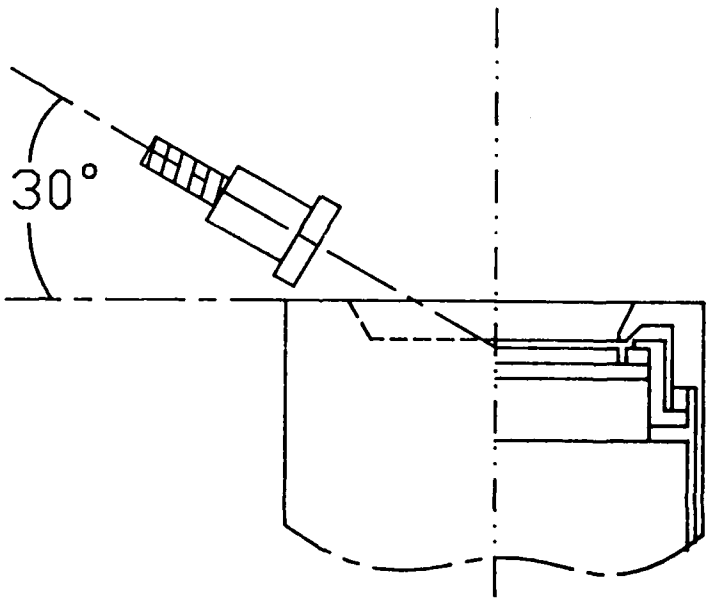


Figure 4. The relative positions of the rotating substrate holder and sputter target are shown.

The proper choice of sputter target composition is essential to the growth of a film of the proper stoichiometry. Although a stoichiometric $YBa_2Cu_3O_7$ sputter target was purchased from Pure Tech, Inc., a commercial vendor, the poor stoichiometry obtained during the initial sputtering made it obvious that a stoichiometric target would not yield a stoichiometric film. Therefore, the production of sputter targets was pursued in-house. Six 3.8 cm diameter targets of different composition were fabricated by the compaction and reactive sintering of $Y_2O_3$, CuO, and $BaCO_3$ powders. In each case three or more mixing, compaction, and sintering cycles were necessary to obtain uniform dense flat targets. Each target was bonded to a Cu backing plate by silver paint to achieve the necessary thermal contact to the target cooling block.

The target and film compositions obtained from this search procedure are noted in Figure 5. The target compositions are derived from the measured amounts of constituents mixed and reacted. The film compositions were obtained by energy dispersive analysis by x-ray in a scanning electron microscope. The sputter gas composition of 98 % Ar/2 % O2 was used with a chamber pressure of 0.8 Pa (6 mTorr). An rf power level of 75 watts over the 3.8 cm diameter target was maintained during presputter and deposition. The difficulties inherent in the Y-Ba-Cu oxygen system are apparent in the spread of compositions obtained from each target. In particular, the compositions of the as-deposited films from any given target were found to be significantly influenced by the total sputter time of the target. Apparently a composition gradient is created in the target during sputtering. Since this gradient forms over a period of several hours of sputter time, a conditioning time of more than ten hours is necessary to obtain a reproducible film composition.

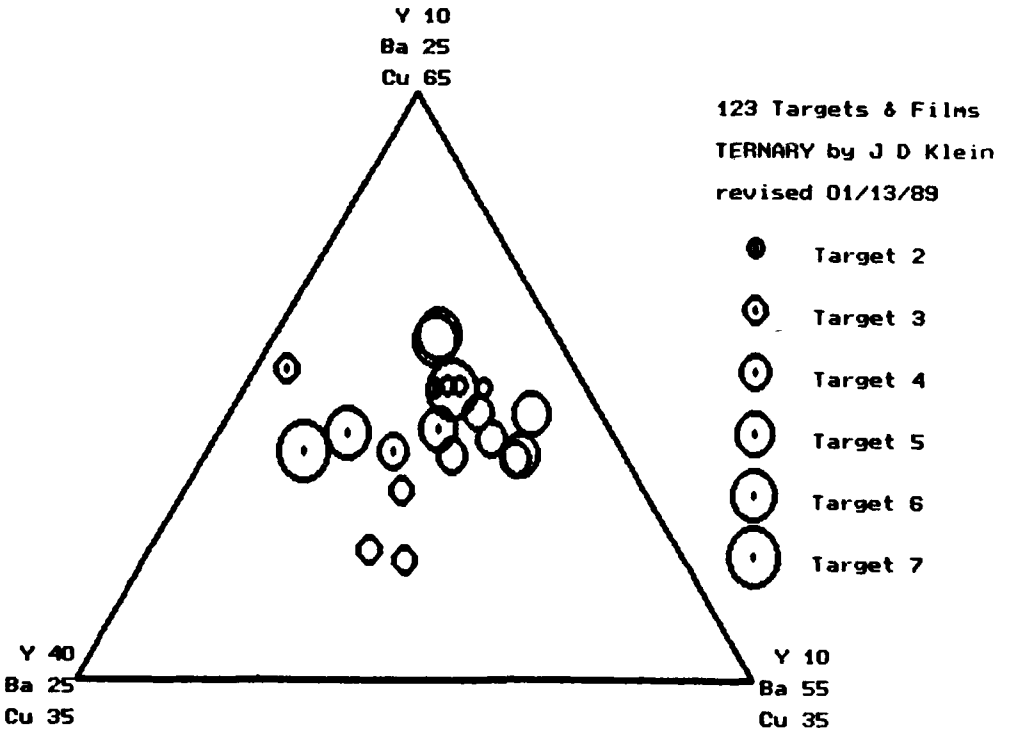


Figure 5. The compositions of six sputter targets and the corresponding as-deposited films are shown on a ternary composition diagram.

The compositions of multiple cation oxides are known to be highly sensitive to sputter deposition conditions. Therefore the exertion of the necessary cation composition control is more than a matter of deducing the proper target composition. Other sputter parameters must necessarily influence the spatial distribution of cation species. To determine the impact of target-to-substrate separation, sputter gas pressure, and sputter power several combinations of conditions were explored by compositional analysis of as-deposited films. This series of films was deposited from target seven after a conditioning sputter period of 12 hours duration. To obtain compositions representing a greater depth of the as-deposited films the analysis by the plasma emission spectroscopy method was employed for these trials. Thickness determinations were performed using a Dek-Tak surface profilimeter.

The influence of substrate position on film composition is shown in Figure 6. Target-to-substrate separations of 34 and 53 mm produced the same composition within the error of the measurement procedure. However, the deposition rate is much more strongly influenced by shifting the substrate back from the target. As shown in Figure 7, the deposition rate at the 34 mm separation is 1.7 times that at the 53 mm separation.

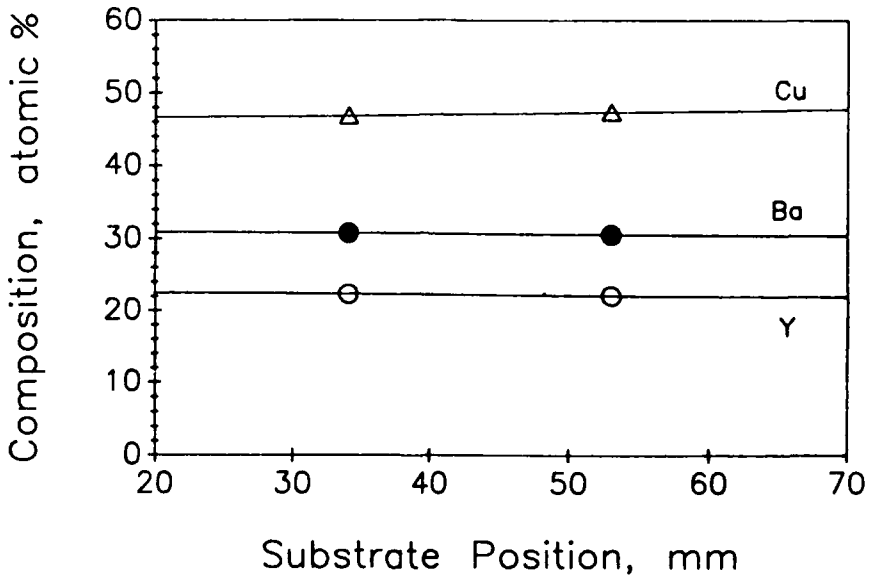


Figure 6. The influence of the center-to-center separation of the target and substrate on composition.

The sputter pressure would be expected to exert a much larger influence on the Y-Ba-Cu composition because it directly influences the characteristics of the sputter plasma. This is indeed the case as can be seen in Figure 8. The higher chamber pressures are associated with greater Y and Ba contents at the expense of the Cu concentration. As such, the ambient pressure provides a means of fine tuning the cation composition of deposited films. As expected, the higher pressures significantly decrease the film growth rate. Over the range of pressures shown in Figure 9, decreasing the sputter pressure enhanced the film growth rate.

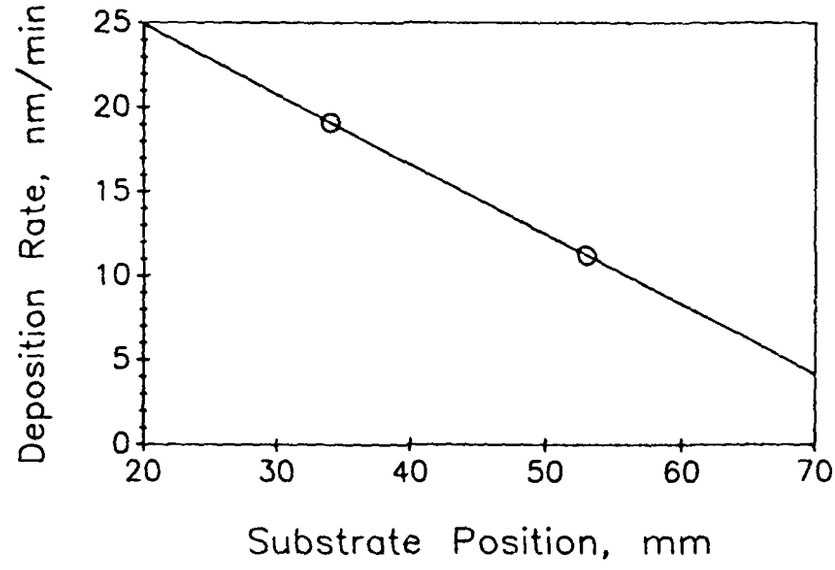


Figure 7. The influence of the center-to-center separation of the target and substrate on deposition rate.

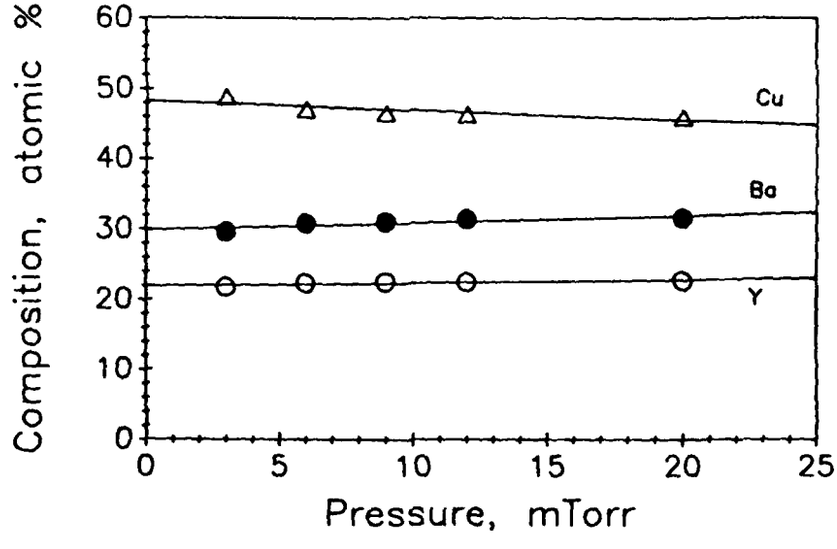


Figure 8. The effect of sputter chamber pressure on the composition of as-deposited films.

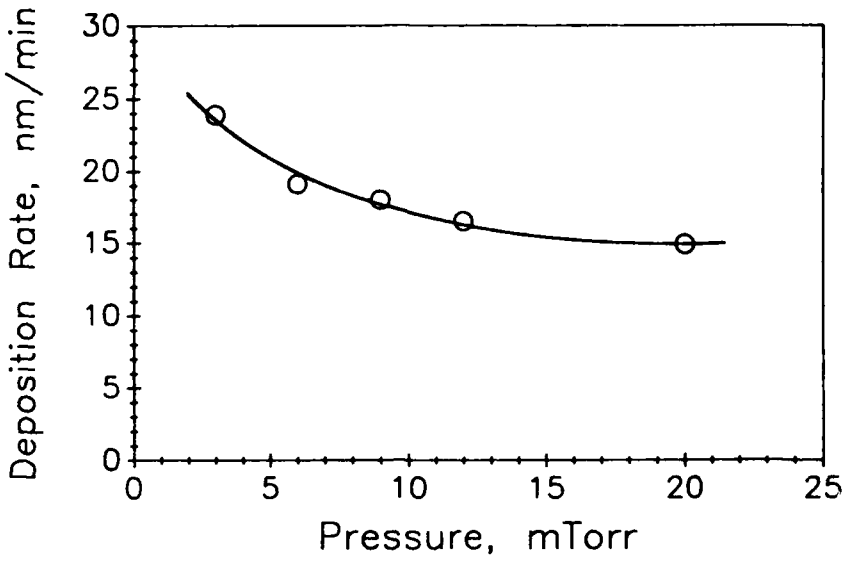


Figure 9. The effect of sputter chamber pressure on the growth rate of as-deposited films.

The rf power would be expected to have the strongest effect on the composition of the films because of its direct control on the shape and intensity of the plasma. Power will influence the composition, energy, and distribution of the cation species. Additionally, by controlling the size and energy of the plasma power significantly determines the degree of negative ion resputtering from the substrate. As seen in Figure 10 the rf sputter power has a much stronger impact on the film composition than was observed for the two previous variables. Increasing the sputter power from 20 to 75 watts increases the Cu content but decreases the Ba composition. Although a linear effect is suggested by the lines shown in Figure 10, the apparently nonlinear composition values depicted for a power of 60 watts were supported by a second independent set of trials with a different target. Also, the deposition rate data of Figure 11 are relatively smooth with respect to power. The increase of film growth rate with increasing power is remarkably linear over the range investigated.

## 2.2 Measurements on Specific Films

The proposed design for a tunable superconducting infrared detector requires a polycrystalline superconducting film in which the transition temperature can be manipulated electrochemically. The electrically controlled action of the oxygen ion conductor is intended to adjust the oxygen content of the superconducting film from a maximum value corresponding to $YBa_2Cu_3O_7$ to values corresponding to $YBa_2Cu_3O_{6.7}$. In this way the transition temperature of the film can be adjusted from more than 90 K to about 60 K. Implementation of the tuning feature therefore requires the development of a film having the desired microstructure and a fully oxidized transition temperature of more than the anticipated liquid nitrogen bath temperature of 77 K.

Most of the early development work determining the proper target composition was performed on MgO substrates. The 2.6 micron thick film shown in Figure 12 was deposited from a stoichiometric target on an unheated single crystal MgO substrate. The sputter power was 75 watts for the 5 cm diameter target in 90 % Ar/10% $O_2$ atmosphere. Although the as-deposited film was

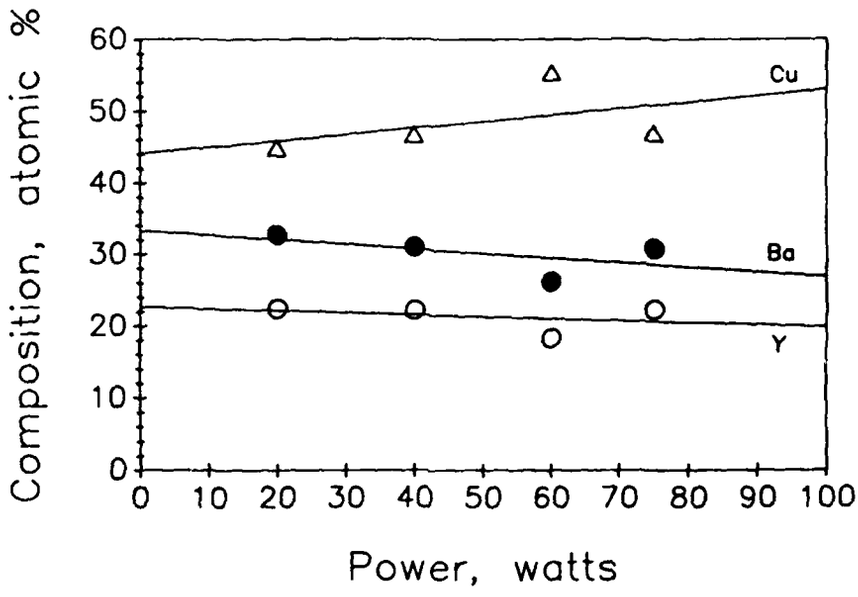


Figure 10. The effect of sputter power on the composition of as-deposited films.

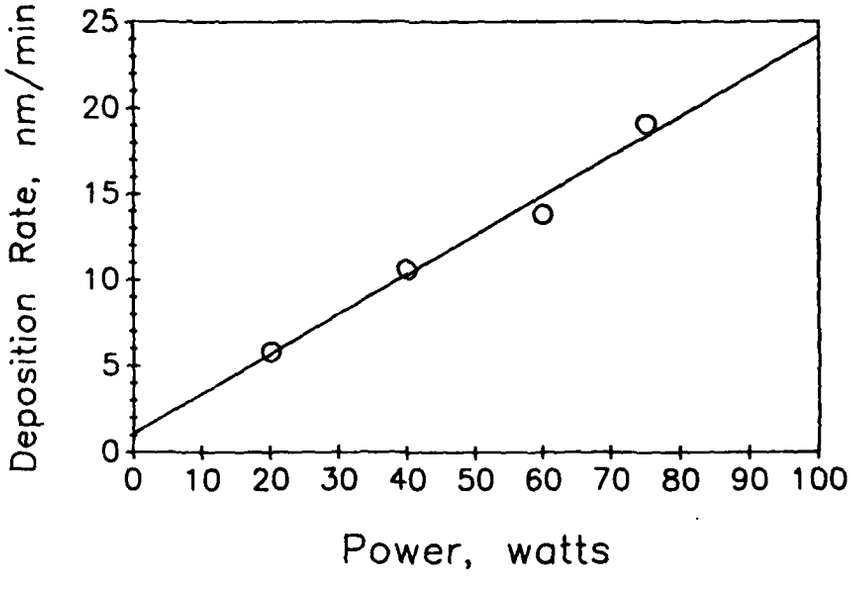


Figure 11. The effect of sputter power on the growth rate of as-deposited films.

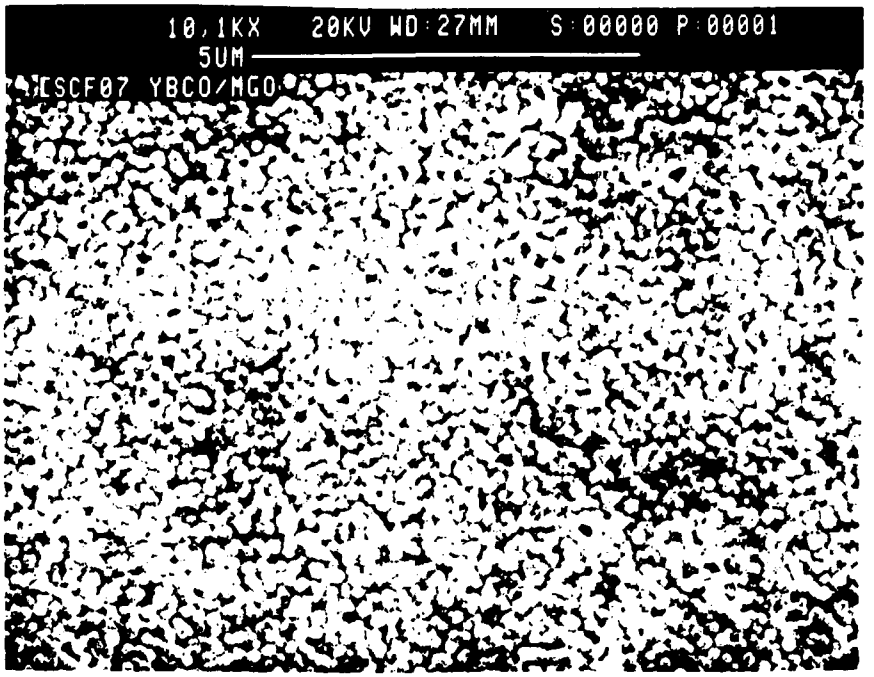


Figure 12. A granular polycrystalline YBCO film deposited on a MgO substrate.

largely noncrystalline a post-deposition heat treatment yielded the granular polycrystalline morphology shown in Figure 11. The heat treatment sequence consisted of a 40 minute ramp from 400 to 650°C, a six hour ramp from 650 to 850°C, and a two hour soak at 850°C followed by furnace cooling. All steps of the treatment were performed in a flowing oxygen atmosphere to fully oxidize the film. Note particularly that the granular morphology is consistent with that originally specified for the prototype detector.

The resistively measured superconducting transition of the YBCO/MgO film is shown in Figure 13. A transport current of ten microamps was continuously passed through the sample while the temperature was controlled by a noninductively wound resistance heater surrounding the sample and the silicon cryodiode thermometer. Temperatures below the 77.3 K liquid nitrogen boiling point were accessed by evacuating the atmosphere above the liquid. Although the onset of the transition is slightly above 90 K, the completion occurs at 70 K. This low completion point implies poor cation stoichiometry in the as-deposited film. The inadequacy of the cation stoichiometry is further supported by the semiconducting behavior indicated by the negative normal state slope above 90 K.

The x-ray diffraction pattern of the 70 K film is shown in Figure 14. Filtered Cu radiation yielded a pattern dominated by the MgO substrate. Besides several peaks attributable to the MgO and the mounting clay, there appears only a single peak attributable to the three strongest reflections from $YBa_2Cu_3O_7$. This indicates that the superconducting film consisted of randomly oriented crystals of poor crystallinity.

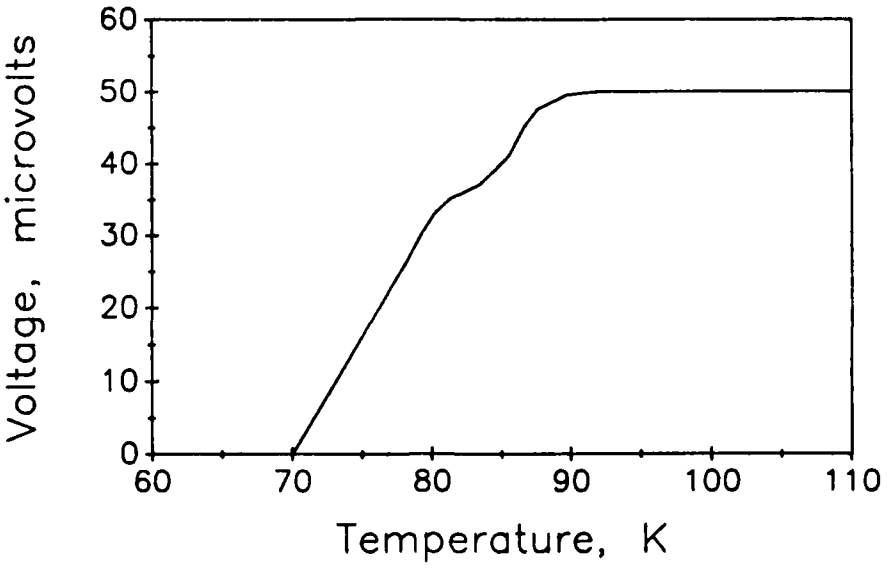


Figure 13. The superconducting transition of the YBCO/MgO film. The sample current was 10 microamps.

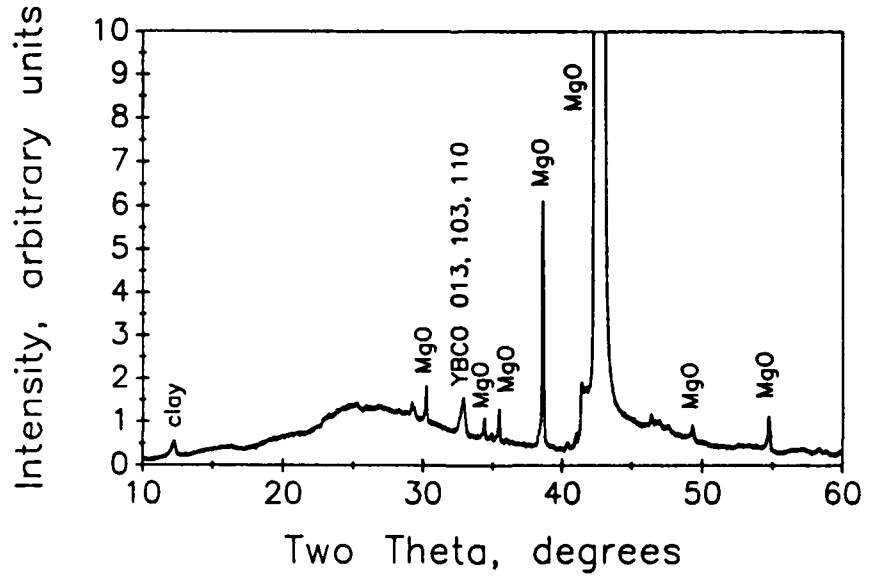


Figure 14. The x-ray diffraction pattern of the 70 K YBCO/MgO film.

The implementation of the tunable design requires the deposition of the superconducting film on an oxygen ion conductor substrate. This project seeks to employ a bare or noble metal coated yttria-stabilized-zirconia (YSZ) monocrystal substrate. After adjusting the target composition with the MgO substrate trials, several films were deposited on (100) oriented single crystal YSZ substrates. A scanning electron micrograph of a heat treated film deposited from target 6 is shown in Figure 15. This film was deposited from a 3.8 cm diameter target rf sputtered at a power of 75 watts in a 98 % Ar/2 %$O_2$ chamber atmosphere maintained at a pressure of 0.8 Pa (6 mTorr). The unheated rotating substrate was maintained at a substrate-to-target center distance of 34 mm. A deposition time of 50 minutes resulted in a one micron thick film. The post deposition heat treatment consisted of a 3 hr ramp from 100 to 900°C, a one hour soak at 900°C, and a fourteen hour ramp from 900 to 100°C. A flowing oxygen atmosphere was maintained throughout the heat treatment to maximize the oxygen content of the film.

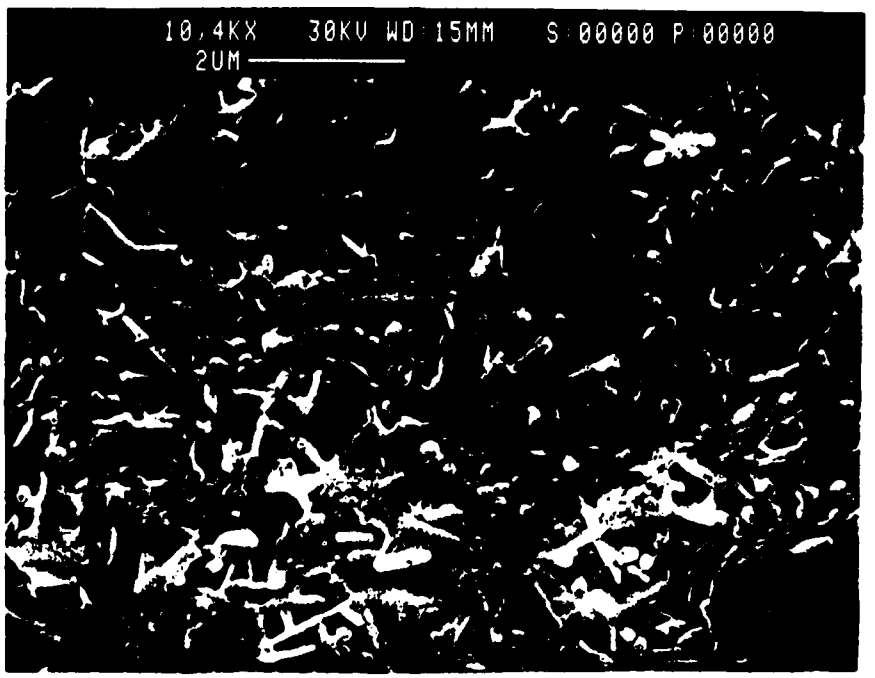


Figure 15. A scanning electron micrograph of a heat treated YBCO/YSZ film.

Although the surface appearance of the film shown in Figure 15 lacks the regular appearance of the previous film, its properties are much more favorable for the intended application. A signal derived from a superconducting device is generally enhanced by higher current levels. In order to more closely simulate anticipated detector operation a current of 10 milliamps was employed to obtain the superconducting transition shown in Figure 16. The linear trace from 290 to 100 K indicates the desired metallic behavior for electrical conduction in the normal state. A transition onset temperature of 95 K suggests that the stoichiometry of much of the film is nearly correct. However, the tailing of the trace to the completion temperature of 81 K indicates that some nonstoichiometric material lies between the grains of good superconductor.

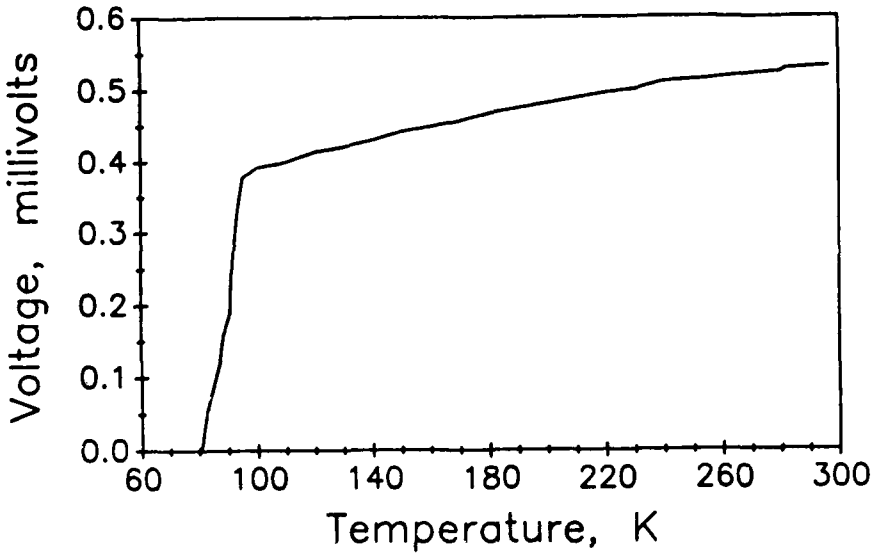


Figure 16. The superconducting transition of the YBCO/YSZ film. The sample current was 10 milliamps.

The x-ray diffraction pattern of the YBCO/YSZ film is particularly encouraging. Filtered Cu radiation was used to obtain the diffractometer scan shown in Figure 17. Besides the expected mounting clay and YSZ substrate peaks there are several YBCO and two In peaks. The indium peaks are from the contacts used to measure the transition temperature. All of the YBCO peaks are (00l) reflection from the $YBa_2Cu_3O_7$ phase. This indicates that the film is comprised of oriented crystals of the superconducting phase. In particular, the (00l) orientation is exactly that which will give maximum critical current in the plane of the film. This is particularly beneficial in that this oriented polycrystalline microstructure provides a film of high critical current density punctuated by grain boundaries susceptible to the formation of weak links under the electrochemical operation of the oxygen ion conductor.

## 2.3 Oxygen Control of Transition Temperature

The tuning process of the detector design requires the motion of oxygen into and out of the superconducting film at relatively modest temperatures. Preliminary trials were performed to demonstrate the feasibility of oxygen motion at temperatures appropriate for ion conductor operation. The 81 K YBCO/YSZ film described in the previous section was subjected to a heat treatment of one hour at 400°C in a vacuum of less than 0.001 Pa. This produced a film that gave no indication of superconductivity down to 66 K. The resistance of the reduced film was relatively constant at 100 ohms compared to the 0.4 ohm resistance indicated in Figure 16 for the normal state of the oxidized film. As can be seen in Figure 18, the x-ray diffraction pattern was significantly altered by the vacuum anneal. Although the same 002, 003, 005, and 006 peaks are present their positions are shifted to lower diffraction angles. This indicates that while the microstructure and crystal orientation were preserved, the size of the unit cell has changed to accommodate the loss of oxygen.

In order to show the reversibility of the oxygen intercalation in the lattice an additional 400°C heat treatment was performed in flowing oxygen to restore the oxygen content of the YBCO lattice. As expected, the oriented polycrystalline microstructure was preserved and the diffraction pattern has been restored to that of a fully oxidized film. The YBCO diffraction peaks shown in

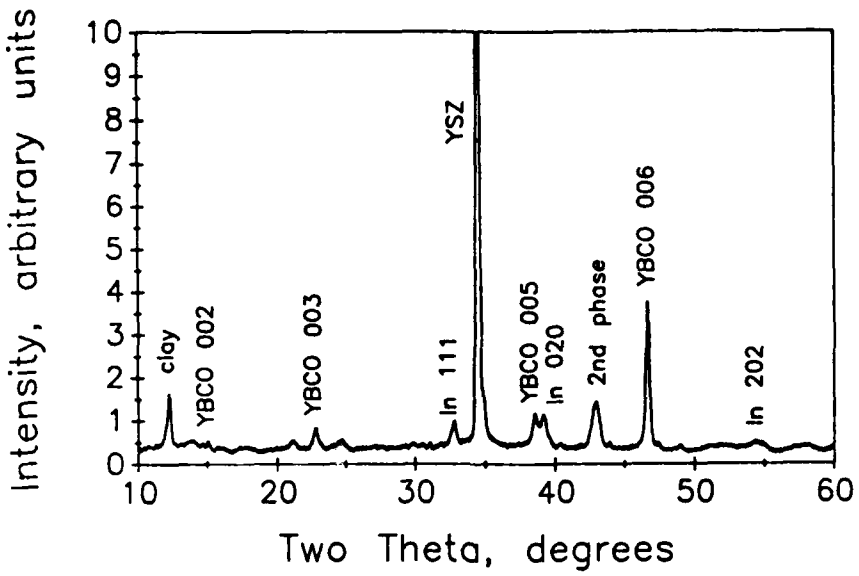


Figure 17. The x-ray diffraction pattern of the 81 K YBCO/YSZ film.

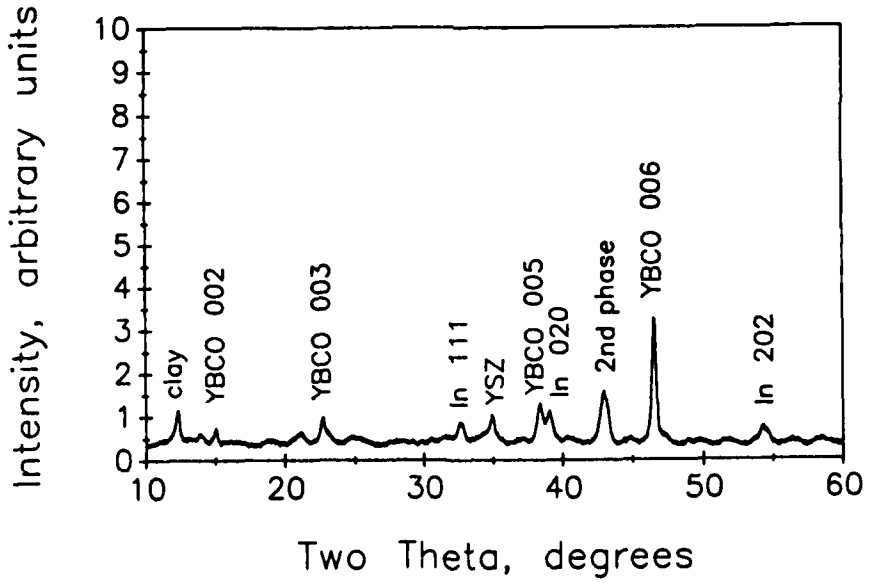


Figure 18. The x-ray diffraction of the YBCO/YSZ film after a 400°C vacuum anneal. The lower oxygen content shifts the YBCO peaks to lower diffraction angles.

Figure 19 lie in almost exactly the same positions they occupied before the vacuum heat treatment. Note however that the diffraction peak of the YSZ substrate has been shifted appreciably from that originally observed for the fully oxidized film. This would seem to indicate that the YSZ substrate had not reached equilibrium with the oxidizing atmosphere. The low temperature oxygen anneal was successful in restoring the superconducting transition to the film. However, the 90 K onset and 63 K completion temperatures have been appreciably depressed by diffusion of the indium contacts into the film.

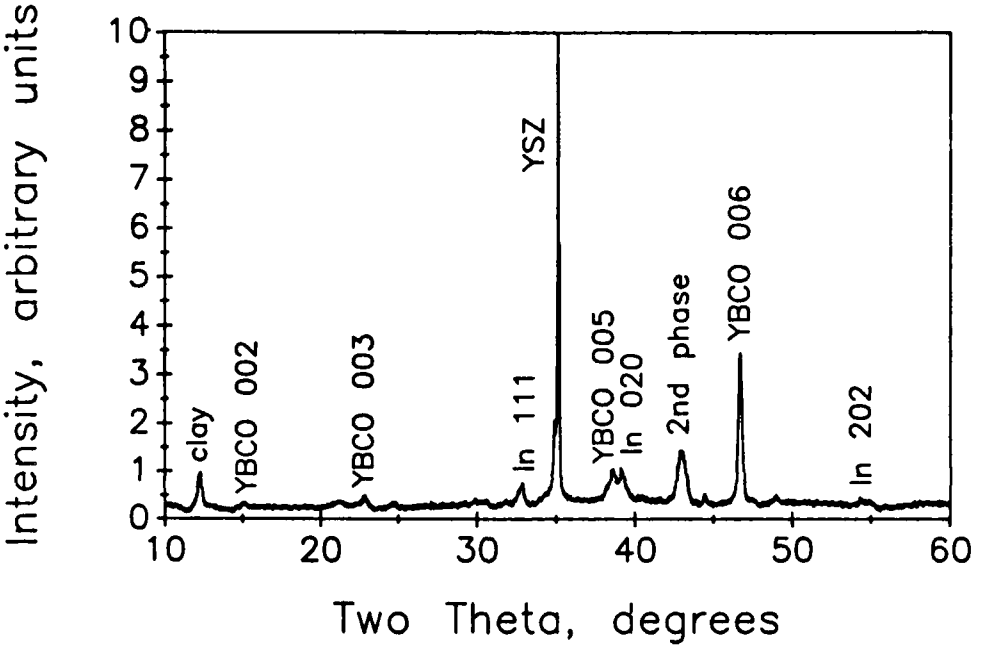


Figure 19. The x-ray diffraction of the YBCO/YSZ film after a 400°C vacuum and flowing oxygen anneals. Restoration of the oxygen content shifts the YBCO peaks to the diffraction angles of the fully oxidized lattice.

Crystal structure is a sensitive measure of the oxidation state of the superconducting films. The intercalation of oxygen in the YBCO lattice causes changes in the lattice parameters of the orthorhombic unit cell. In the present case of an oriented films with the c-axis perpendicular to the substrate surface only the 002, 003, 005, and 006 diffraction angles are available for lattice calculations. The diffraction angles measured for these peaks are recorded for the different anneal conditions in Table 1. Since each of these 00*l*-type planes lie parallel to the a-b plane of the YBCO unit cell, their interplanar spacings give information only about the c lattice parameter. Through the use of proprietary software a least squares extrapolation fit has been performed to determine the influence of the oxidation state on the c parameter. The fully oxidized films produced by oxygen atmosphere annealing at 900 and 400°C have a c lattice parameter of 11.64 Angstroms. In contrast, removal of oxygen from the YBCO unit cell by the 400°C vacuum anneal shifts the c parameter to 11.69 Angstroms. Thus, it is readily apparent that 400°C provide the desired oxygen mobility in both the YSZ and YBCO lattices.

Table 1. Annealing conditions, diffraction angles, lattice parameters, and transition temperatures for a YBCO/YSZ film given sequential heat treatments.

| last anneal temperature, °C | 900 | 400 | 400 |
|---|---|---|---|
| last anneal atmosphere | oxygen | vacuum | oxygen |
| 0 0 2 peak angle, degrees | 15.05 | 15.00 | 15.07 |
| 0 0 3 peak angle, degrees | 22.76 | 22.67 | 22.76 |
| 0 0 5 peak angle, degrees | 38.53 | 38.32 | 38.55 |
| 0 0 6 peak angle, degrees | 46.63 | 46.51 | 46.65 |
| c lattice parameter, Angstroms | 11.643 | 11.689 | 11.644 |
| Transition onset Temperature, K | 95 | <66 | 90 |
| Transition Completion Temperature, K | 81 | <66 | 63 |

## 2.4 Control of Grain Size

The use of a polycrystalline microstructure to define the weak links permits the scale of the junction network to be controlled by manipulation of the grain size of the superconducting phase. As is the case with other polycrystalline microstructures the grain size can be varied through careful choice of annealing temperature. In the present films this effect is demonstrated by considering two films having histories that differ only in heat treatment. Both films were sputtered from Target 7 at a power of 75 watts with a chamber pressure of 0.8 Pa (6 mTorr). The film shown in Figure 20 was given a flowing oxygen heat treatment comprised of a two hour ramp from 400 to 650°C, a 6 hour soak at 650°C, a one hour ramp from 650 to 860°C, and a one hour soak at 860°C followed by furnace cooling. As can be determined by examination of the scale of the microstructure in the right part of the image, the average grain size is approximately 0.3 microns. Note also the presence of a large particle of second phase material in the upper left corner of the picture. The segregation of the film into different phases during heat treatment allows continuous superconducting paths to exist in films having average compositions that are not stoichiometric.

In contrast, the film shown in Figure 21 was given an identical heat treatment except for the use of 900°C for the high temperature portion of the heat treatment. The average grain size in Figure 21 is more than 0.5 microns. Thus the scale of the microstructure can be varied through variations in post deposition anneal conditions.


Figure 20. A scanning electron micrograph showing the relatively fine grain size in a YBCO/YSZ film heat treated at a maximum temperature of 860°C.


Figure 21. A scanning electron micrograph of the large grain size in a YBCO/YSZ film heat treated at a maximum temperature of 900°C.

## 3.0 TECHNICAL FEASIBILITY

The Phase I program was successful in demonstrating the fabrication of a thin film microstructure appropriate for incorporation in a tunable infrared detector. Specifically, an oriented polycrystalline superconducting $YBa_2Cu_3O_7$ thin film was deposited on an yttria stabilized zirconia oxygen ion conductor substrate. Reduction of the oxygen content in a low temperature (400°C) vacuum anneal was successful in reducing the transition onset temperature from 95 K to less than 66 K. Reoxidation in a flowing oxygen atmosphere restored the superconductivity and the lattice parameters of the film.

The success of oxygen ion conductor substrates in tuning the response of infrared detectors depends on the predictable manipulation of the superconducting properties of a thin film junction structure. The Phase I program has demonstrated the potential for the relatively low temperature adjustment of the superconducting transition offset temperature of an oriented polycrystalline thin film from 95 K to less than 66 K. It is especially important that a thin film microstructure appropriate for the desired junction array was achieved on the YSZ substrate. The development of a crystallographically oriented polycrystalline film can be expected to enhance the available detector speed and sensitivity by providing a high critical current film punctuated by narrow through-film weak links. Based on the reported oxygen transport properties of $YBa_2Cu_3O_7$ and yttria stabilized zirconia, the desired reversible electrochemical redox reaction should be possible at temperatures as low as 350°C.

Most approaches to superconducting infrared detectors involve the necessary development of junction characteristics through the patterning of epitaxial single crystal films. The drawbacks of such approaches are the introduction of insulating phases during patterning, the unavailability of post deposition tuning, and difficulty in incorporating gradient structures. In contrast, the oxygen ion conductor based detector has a number of inherent advantages:

- Minor deficiencies in cation stoichiometry are tolerated by the segregation of insulating phases.
- The utilization of a polycrystalline microstructure relaxes the deposition requirements.
- The oxygen ion conductor will permit exacting control of the transition temperature of the weak links in the film by adjusting their oxygen stoichiometry without the need for stringent atmosphere control.
- The creation of gradient structures within the superconducting film can be accomplished by the application of a voltage gradient across the plane of the superconducting film.

The proposed Phase II program would be concerned with demonstrating precise control of the superconducting properties of the thin film structure by electrochemical means, defining the response to infrared radiation, and more precisely determining deposition conditions appropriate for developing a fully oxidized polycrystalline film with superior transport properties. In the latter half of the program emphasis would be placed on incorporating the proposed technology into practical detection devices.

## 4.0 REFERENCES


1. M. Leung, P. R. Broussard, J. H. Clausen, M. Osofsky, S. A. Wolf, and U. Strom, Appl. Phys. Lett. 51 2046 (1987).

2. M. G. Forrester, M. Gottlieb, J. R. Gavaler, and A. I. Braginski, Appl. Phys. Lett. 53, 1332 (1988).

3. H. S. Kwok, "Nonthermal Optical Response in YBCO", MRS Meeting, Boston, November 1988, Abstact F.10.

4. P. M. Mankiewich, R. E. Howard, W. J. Skocpol, A. H. Dayem, A. Ourmazd, M. G. Young, and E. Good, "High-Critical-Current-Density Thin Films of $Ba_2YCu_3O_7$ Produced by Coevaporation of Y, Cu, and $BaF_2$," MRS Meeting, Boston, November 1987, Abstract AA3.11.

5. R. A. Laudise, L. F. Scheemeyer, and R. L. Barns, J. of Crystal Growth 85, 569 (1987).

6. D. S. Ginley, E. L. Venturini, J. F. Kwak, R. J. Baughman, B. Morosin, and J. E. Schirber, Phys. Rev. B 36, 829 (1987).

7. U. Dai, G. Deutscher, and R. Rosenbaum, Appl. Phys. Lett. 51, 460 (1987).

8. H. Kamukura, M. Uehara, and K. Togano, Appl. Phys. Lett. 51, 1557 (1987).

9. P. Chaudhari, D. Dimos, and J. Mannhart, "Grain Boundary Critical Currents in $YBa_2Cu_3O_7$," MRS Meeting, Boston, November 1988, Abstract F4.8.

10. S. Hatta, H. Higashino, K. Hirochi, H. Adachi, and K. Wasa, Appl. Phys. Lett., 53, 148 (1988).

11. R. A. Laudise, L. F. Scheemeyer, and R. L. Barns, J. of Crystal Growth 85, 569 (1987).

12. E. M. McCarron, R. K. Bordia, J. P. Attfield, C. C. Torardi, and A. W. Sleight, Materials Research Society 1987 Fall Meeting, AA3.6 (1987).

13. E. Hamann, H. Manger, L. Steinke, SAE Trans. 86, 807 (1975).

14. N. M. Beekmans and L. Heyne, Philips Technical Review 31, 112 (1970).

15. B. T. Ahn, T. M. Gur, and R. A. Huggins, Materials Research Society 1987 Fall Meeting, AA5.8 (1987).

16. K. N. Tu, S. I. Park, and C. C. Tsuei, Appl. Phys. Lett., 51 2158 (1987).

17. R. L. Sandstrom, W. J. Gallagher, T. R. Dinger, R. H. Koch, R. B. Laibowitz, A. W. Kleinsasser, R. J. Gambino, B. Bumble, and M. F. Chisholm, Appl. Phys. Lett. 53, 444 (1988).

## REPORT DISTRIBUTION LIST

| | |
|---|---|
| Commander<br>U.S. Army Missile Command<br>ATTN: AMSMI-RD-DP-TT/Dr. Charles R. Piner<br>Bldg 7770 Rm 107<br>Redstone Arsenal, AL 35898-5244 | 1 Copy |
| Commander<br>U.S. Army Missile Space and Intelligence Center<br>ATTN: AMSMI-RD-CS-R<br>Redstone Arsenal, AL 35898-5240 | 1 Copy |
| Commander<br>U.S. Army Missile Command<br>ATTN: AIAMS-YDL<br>Redstone Arsenal, AL 35898-5500 | 1 Copy |
| Commander<br>U.S. Army Missile Command<br>ATTN: AMSMI-RD-RE<br>Redstone Arsenal, AL 35898-5248 | 1 Copy |
| Director<br>Defense Advanced Research Projects Agency<br>ATTN: Dr. Lupo<br>1400 Wilson Boulevard<br>Arlington, VA 22209-2308 | 1 Copy |
| Director<br>Defense Advanced Research Projects Agency<br>ATTN: TIO<br>1400 Wilson Boulevard<br>Arlington, VA 22209-2308 | 1 Copy |
| Defense Technical Information Center<br>ATTN: DTIC-DDR<br>Alexandria, VA 22304-6145 | 2 Copies |